SP 162-13

Ductile Connections for Precast Concrete Frame Systems

by L. Palmieri, E. Saqan, C. French, and M. Kreger

Synopsis: This paper describes a research program to investigate the behavior of ductile connections between precast beam-column elements. Eight beam-column connections were tested to characterize the overall behavior of the connection details. Each connection specimen was designed to incorporate one of three behavioral concepts in the connection elements: tension/compression yielding, substantial energy dissipation, or nonlinear-elastic response. Based on the behavioral information collected during connection tests, analytical models were developed to investigate the behavior of complete precast frame systems. Results of the experimental study and preliminary results of the analytical work are presented. The objective of the program is to provide rational design recommendations for engineers to detail precast frame connections for use in regions of seismic risk.

Keywords: Connections; ductility; earthquake-resistant structures; energy; frames; friction; joints (junctions); precast concrete; unbonded post-tensioning

Lucio Palmieri is a Doctoral Candidate and Research Assistant at the University of Minnesota. He received his Diploma in Civil Engineering at the Universita' di Bologna, Bologna, Italy, and his M.S. from the Department of Civil Engineering at the University of Minnesota.

Elias I. Saqan is a former graduate research assistant at the University of Texas at Austin. He received a B.S. from the University of Houston in 1989, and received M.S. and Ph.D. degrees in Civil Engineering from the University of Texas at Austin in 1991 and 1995.

Catherine French, FACI, is an Associate Professor of Civil Engineering at the University of Minnesota, Minneapolis. She is a member of ACI 318, 352 Joints in Monolithic Concrete Structures, 368 Earthquake Resisting Elements and Systems, 423 Prestressed Concrete, and secretary of 445 Shear and Torsion.

Michael E. Kreger is an Associate Professor of Civil Engineering at the University of Texas at Austin. He is chair of ACI-ASCE Committee 352, Joints in Monolithic Concrete Structures. He is a member of ACI 318-H Seismic Provisions, and 368 Earthquake Resisting Elements and Systems.

INTRODUCTION

Precast concrete construction represents an attractive and economical solution for many types of multistory buildings. Advantages of precast concrete over cast-in-place concrete include superior quality control, speed of erection, and aesthetic architectural form. However, relatively few precast structures are constructed in seismic areas of the United States because framing methods and current connection details between precast elements suitable for use in U.S. construction practice are not explicitly approved in design codes. The current 1994 Uniform Building Code (UBC) classifies precast frame systems, such as those discussed in this paper, as an "undefined structural system" (1). In order to utilize such a structural system, the UBC requires that the lateral-force resistance and energy absorption capacity for this "undefined structural system" be shown by technical and test data to be equivalent to one of the structural systems defined in the code. In effect, current UBC provisions require that precast frames emulate a cast-in-place reinforced-concrete system.

The coordinated research effort "Precast Structural Seismic Systems" (PRESSS) was initiated to address this need. The ultimate objectives

of the program are to develop precast concrete systems and corresponding design recommendations for seismic regions. The program has sought innovation, taking advantage of the unique characteristics of U.S. precast construction to provide economical building systems. With this philosophy, the research has focused primarily on development of systems which use ductile connection concepts for concrete frame and panel systems. The connections themselves are designed to accommodate most of the lateral deformation, while the precast members remain relatively undamaged. This approach is in sharp contrast to precast construction practice in Japan where buildings are designed using substantially different details and essentially the same design philosophy as is used for cast-in-place concrete buildings (2). Reinforcement details that are substantially different from those used in monolithic construction are used to accommodate connections between the precast members, but the final product has been shown to behave very similar to cast-in-place construction. Because of this, the Japanese precast design approach has been referred to as "emulation design". Earlier research (3,4) conducted in New Zealand during the 70's examined the cyclic behavior of precast, prestressed beam-column connections. Blakeley and Park recognized the obvious deformation capabilities inherent in precast, prestressed connections. However, even though these connections were not intended to "emulate" cast-in-place connection behavior, specimen response was evaluated using cast-in-place behavior as the reference. Similar precast, prestressed specimens discussed in this paper were designed and evaluated with quite different behavioral objectives in mind.

This paper describes the portion of PRESSS research conducted at the University of Minnesota (UMn) and The University of Texas at Austin (UT) to evaluate the behavior of ductile connections between precast beam-column frame elements. The research was divided into three major components:

(1) Development of Ductile Connection Details
(2) Experimental Investigation of Beam-Column Subassemblages
(3) Analytical Modeling of Precast Systems.

DEVELOPMENT OF DUCTILE CONNECTION DETAILS

In this phase of the project, a variety of ductile connection details were developed in cooperation with industry representatives. The details may be grouped into four behavioral categories: tension/compression yielding, energy dissipating, nonlinear-elastic, and shear yielding. Conceptual examples of different connection types are shown in Fig. 1. The first five details (Fig. 1(a)-(e)) represent connections which would dissipate energy through tension and compression yielding of the

connection elements.

Figure 1(f) shows an example of an energy-dissipating device. In this case, energy is dissipated through friction. Holes are slotted in the plates to accommodate the anticipated drifts without bolts going into bearing. Special materials may be used to enhance the friction coefficient.

Figure 1(g) illustrates a nonlinear-elastic connection (depicted by thickened beam end regions, referred to as horizontal "dogbones," with central post-tensioning). The detail was derived from a concept proposed by Priestley and Tao (5). The connection is constructed with unbonded post-tensioning reinforcement located close to beam middepth, and is detailed to maintain reinforcement stresses below the proportional limit during a design-level earthquake. The connection derives its name from characteristics of the associated story shear versus drift response. When the story shear attains a level sufficient to open the joint between each precast beam and the column, the response deviates from the original linear-elastic behavior. Even though behavior becomes nonlinear due to large deformations at the joint interface, the post-tensioning steel remains elastic during design-level events. The still elastic unbonded post-tensioned reinforcement causes the connection to return to its undeformed position when story shear is reduced to zero. The National Institute of Standards and Technology (NIST) has conducted a variety of tests on centrally post-tensioned connections that incorporate mild reinforcement details (6,7).

The shear-yielding concept, shown in Fig. 1(h), was investigated by Popov in steel frames employing eccentric bracing (8). The rigidity of the concrete frame may promote the development of shear yielding in a structural steel element similar to that observed in an eccentrically braced steel frame. The connection in Fig. 1(h) is shown in its original and deformed configuration.

EXPERIMENTAL INVESTIGATION OF SUBASSEMBLAGES

To characterize the behavior of the connection details, one-half scale precast beam-column subassemblages were fabricated and tested under reversed cyclic loads. The subassemblages were scaled from a system developed by PRESSS Phase I researchers at Englekirk and Sabol Consulting Engineers, Inc. The floor plan for the prototype structure is shown in Fig. 2. Lateral-force-resisting elements in this building are concentrated along the perimeter of the frame. Because the connections are intended to resist lateral force reversals along one direction, connection subassemblages were subjected to unidirectional reversed cyclic loads.

The one-half scale test specimens represented interior beam-column joints located in the lower stories of the peripheral frame spanning in the short direction of the 15-story prototype structure (also shown in Fig. 2). The required nominal moment capacities for the connections tested in this study were scaled from the prototype structure. The design moment M_u, for the prototype structure was 2283 ft-k; the calculated one-half scale design moment was 285 ft-k. A strength reduction factor of 0.9 was used to obtain the nominal moment capacity, M_n, of 317 ft-k. The story drift level (ratio of story lateral displacement and story height) under the nominal moment M_n was targeted to be 2 percent.

The nominal "loading" history is shown in Figure 3. The subassemblages were taken to increasing drift levels comprising the following sequence: one cycle each at 0.05, 0.075, and 0.1% drift, followed by three cycles each at 0.25, 0.5, 0.75, 1, 1.5, 2, 2.5 and 3% drift. After each set of three cycles, an intermediate cycle was imposed to a peak load of 75 percent of the previously attained peak load to investigate stiffness degradation. Some specimens were subjected to additional deformations of two cycles at 4% drift, one cycle each at 5, 6, and 7% drift and a final monotonic displacement to 10% drift. For convenience, desired drift levels were applied to specimens by vertically displacing the beam tips in opposing directions (Fig. 4a) rather than by laterally displacing the top of the column.

A total of eight beam-column subassemblages, representative of three of the four connection categories, were tested. An example of the shear yielding concept was not included in this study.

Tension-Compression Yielding Concept

Four of the connections tested represented examples of the tension-compression yielding concept: UT specimens GAP and DB; and UMn specimens GAP and TCY.

UT-GAP was representative of the "gap-joint system" which received very favorable reviews from the precast industry advisory group (Fig. 5). In the gap-joint system, the beam is intended to be restrained from translation at the bottom (or top) of the beam-column interface. Lateral movement is accommodated by rotation about that point through opening and closing of a gap (1 in. wide in this specimen) at the top (or bottom) of the interface. The gap system is desirable for two reasons: (1) It enables ease of fabrication of the bottom connection; the erectors can lower the beam into place and complete both the top and bottom connection while working from the top of the beam. (2) If the gap is provided at the bottom of the beam, the lack of translation at the

top surface will prevent large cracks from developing across the floor panels at the beam-column interface under cyclic lateral loading. In the tension/compression yielding type connections, the gap at the interface of the beam and column permits both tension and compression yielding of the connecting elements.

Specimen UT-GAP incorporated tapered threaded couplers in the column to mate with mild reinforcement in the cast-in-place topping of the beam. The bottom horizontal connection and resistance to beam-end uplift were provided by four high-strength vertical rods anchored in the corbel. Oversized holes in the beam provided sufficient construction tolerance to slip the beam ends over the rods. Following placement of the beams, nuts were fastened to the ends of the rods, then the voids around the rods were grouted. Each beam was seated on a neoprene pad to accommodate the rotation of the beam without causing damage to the corbel. Fiber-reinforced grout was placed in the bottom of the gap between the beams and column to facilitate direct transfer of compression forces from the bottom of each beam to the column. The tops of the beams were cast after the beam top bars were screwed into the threaded couplers embedded in the columns.

Response of the specimen is illustrated in Fig. 6 using story shear versus drift. Overall response of the connection was reasonably good through cycles to 2.5% drift. However, some pinching of the hysteresis loops was evident with the onset of inelastic behavior at approximately 0.6% drift. Most of the pinching was attributed to shear and flexural deformations that occurred in the vertical rods at the interface between the corbels and beams. This slip between the two members is indirectly demonstrated in Fig. 7 by the moment-rotation response of one of the beams. Note that stiffness was generally less for loading in the positive-moment direction (which corresponded with opening of the gap at the bottom of the beam). Deformation of the vertical rods at the beam/corbel interface became more pronounced at higher deformation levels and eventually dominated the response. Failure of specimen UT-GAP occurred as the result of fracture of the vertical rods during cycles to 3% drift (note strength reductions in Fig. 6). The compliant bottom connection also affected the inelastic response of the beam top bars which were intended to experience most of the inelastic action in the connection. Figure 8 illustrates the stress-strain response of a beam top bar at the face of one of the beams. Note the tensile inelastic strains (corresponding with opening of the gap at the top of the beam) were substantially greater than compressive inelastic strains. This observation will play a critical role in interpreting the behavior of Specimen UMn-GAP discussed later.

UT-DB employed vertical "dogbones" and high-strength threadbars to

connect precast beams and columns (Fig. 9). High-strength fiber reinforced grout was placed between the beam ends and the column before the beams were connected to the column. Ducts that contained the threadbars were grouted after the threadbars were snug tightened. The story shear versus drift response is illustrated in Fig. 10. Connection behavior was reasonably acceptable through 1% drift cycles, although the high-strength threadbars resulted in less energy dissipation than would be anticipated for monolithic beam-column connections. During loading in the positive direction to 1.5% drift, concrete located between the 90 degree hooks on the longitudinal beam reinforcement and the anchor plates at the ends of the dogbones crushed. The same behavior was observed at approximately 2% drift when the connection was loaded in the negative direction.

The use of connections that provided an indirect path for force transfer between precast elements was the common thread that precipitated the premature failure of specimens UT-GAP and UT-DB.

UMn-TCY was a simple system that incorporated block-outs through the beams and embedded corrugated pipes in the column to accommodate placement of reinforcement. Many of the other connections investigated required the use of couplers or other arrangements which caused discontinuities in the load path. With this system, it was intended to avoid the use of couplers by placing continuous reinforcement in the beam block-outs which could be slid through the column during construction, tied in place, and subsequently grouted. The beam reinforcement could be spliced at midspan near the inflection point for reversed cyclic load. The connection reinforcement was designed to yield at the beam-column interface. The transverse beam reinforcement was increased by approximately 30% (No. 3 bars at 3.5 in.) with respect to the calculated minimum amount (No. 3 bars at 5 in.) to increase the confining action on the longitudinal beam bars, and therefore reduce the possibility of buckling of the bars after reaching yielding. The specimen is shown in Fig. 11. The transverse reinforcement and horizontal skin steel is shown only on the East Beam for clarity. The cross-hatched areas in the beam cross section represent the block-out regions which were grouted after placing the connection reinforcement.

Figure 12 shows a plot of story shear versus drift. Specimen UMn-TCY performed quite well for the design level and up to nominal drifts exceeding 4% (actual drift 3.6%); the peak story shear was reached during the first cycle at 4% nominal drift. At nominal drifts of 5 and 6% the corresponding maximum attained story shear did not show any significant sign of decreasing with respect to the peak story shear attained at 4%. The story shear-drift curves show significant signs of

pinching in the latter part of the test (above 4% drift) which can be attributed to several factors: a) slip between the corrugated pipes housing the longitudinal beam reinforcement (grouted within the pipes) and the surrounding column concrete, b) buckling of the longitudinal beam reinforcement in the connection region close to the beam column interfaces, with consequent spalling of the concrete cover in the beam top and bottom surfaces, and c) relative vertical movement (slip) between column and beams as a result of the elongation, due to yielding, and kinking of the beam longitudinal reinforcement.

Strain gage data indicated that yielding of the beam longitudinal bars occurred at locations corresponding to the beam-column interfaces at nominal drift values of about 1.5%.

UMn-GAP was another example of a tension/compression yielding gap-joint system. The connection is shown in Fig. 13. In this case, the bottom connection was made using two lightly post-tensioned bars (Area / bar = 1.25in.^{2}) each stressed to 94 kips/bar. Although not as easy to erect in the field as the gap system with the vertical rod (UT-GAP), the horizontal element was more efficient in carrying the large horizontal restraining force (200 kips). The post-tensioned bottom reinforcement prevented relative opening of the bottom face of the connection and provided a pivot point for the beam rotation. The post-tensioning was used to provide sufficient clamping force to sustain gravity and lateral shear loads while ensuring the post-tensioning bars would not undergo inelastic deformation during the loading history. Nearly all the deformation was concentrated at the top of the connection through tension and compression yielding of three No. 9 reinforcing bars which were connected through couplers at the beam-column interface.

Because of the longitudinal beam reinforcement buckling experienced during the test of UMn-TCY, the beam transverse reinforcement was increased by 75% (No. 3 bars at 2 in.) in the beam within 1 ft. of the beam-column interface. In the post-tensioned regions at the beam ends additional spiral reinforcement was used to increase the concrete compressive strength and deformability.

The connection was assembled as follows: grout was applied and cured within approximately the bottom third of the beam-column interface; the bottom connecting rods were lightly post-tensioned; the beam top reinforcement was threaded into the couplers cast through the column, and the beam block-outs were grouted. The couplers were threaded after post-tensioning to ensure that no significant initial stresses were induced in the beam top reinforcement. A 1 in. wide gap was left open over the top approximately two-thirds (14 in.) of the beam-column

interface. The beam longitudinal top reinforcement, left exposed in the gap region, was intended to yield in tension and compression under cyclic loading. With increasing levels of applied deformation, the inelastic behavior of the reinforcement would eventually propagate into the beam. Another feature anticipated with the use of the "gap concept" was the limitation of concrete deterioration under reversed cyclic loading. Under imposed deformations the gap should be able to accommodate relative rotations between beams and column, therefore limiting the amount of concrete damage in the beam and column members.

Specimen UMn-GAP performed satisfactorily up to 2% nominal drift. Figure 14 shows the plot of story shear versus drift. The hysteretic behavior of the connection indicates good energy dissipation characteristics as the specimen was subjected to load cycles into the inelastic range. While cycling at the 2% imposed drift level, however, the top reinforcement across the beam suffered a brittle fracture at the beam-column interface, at the face of the couplers. Failure occurred first on the east side of the connection, then after two more cycles on the west side. Data obtained from strain gage measurements show that yielding of the reinforcement was not limited to the gap region, but did propagate within the beam over a region varying between one and two feet. The couplers used were the same type as those used in UT-GAP which experienced 3% drifts before a different connection component failed. However, Fig. 8 demonstrated that the inelastic tensile demand on beam top bars in UT-GAP was much greater than the inelastic compressive demand. Because the bottom connection in UMn-GAP behaved as intended, it is quite likely that much greater inelastic demands (perhaps approximately equal tensile and compressive demands) were imposed on the beam top bars in this specimen than on bars in UT-GAP.

A series of tension tests was conducted on the same reinforcement bars as those used in the specimen, and on bars and coupler assemblages. The results indicated that tensile failures in bars connected with the couplers are not as ductile as those observed for individual bar tests. It should be noted that in all cases the ultimate loads carried by the bar plus coupler assemblages were greater than the loads required by the specifications.

The performance of the post-tensioning rods, comprising the bottom connection, was satisfactory. It appears that the beam rotated about the post-tensioning centroid as anticipated. Very little concrete damage was observed in beam and column members in the connection region.

Energy Dissipating Concept

UT-FR was the only connection tested in this program that incorporated special connection hardware to enhance the energy dissipation capacity of the beam-column connection. The connection details are illustrated in a schematic shown in Fig. 15. The top of each beam was connected to the column by a steel plate assembly that was embedded in the beam and bolted onto the side of the column. The plate assemblies contained 4 in. slotted holes that permitted sliding along vertical plate surfaces on the sides of the beams. Consistency in the level of force required to cause sliding along these plate surfaces was obtained by placing 1/8 in. thick brass plates between all sliding surfaces. The friction coefficient for brass sliding on steel was approximately 0.2. The force required to cause slip on these plate surfaces was controlled by the clamping force applied to the plates which was maintained relatively constant by placing conical (belleville) washers beneath the high-strength bolts that clamped the plates together. The concept for this friction connection stemmed from work conducted by Gregorian, Yang and Popov (9).

The bottom connection between the beams and column was developed to replace the corbel which performed relatively poorly in UT-GAP. Note that the bottom connection shown in Fig. 15 provided a direct path for force transfer from the bottom of the beams into the column, as well as a much more aesthetically pleasing detail. Three 1-1/8 in. diameter A490 bolts were used to connect the bottom of each beam with the corbel. The line of bolts was also intended to act as a pivot point for beam rotation.

Specimen UT-FR behaved quite well through the first two cycles to 3% drift (see story shear versus drift response in Fig. 16). Energy dissipation was enhanced, as intended, and was substantially greater than for any of the other specimens tested in this study. Testing was terminated during the third cycle to 3% drift because a weld between plates in one of the top connections failed as a result of larger than anticipated forces being developed in the connections. It was anticipated that the hysteresis loops shown in Fig. 16 would resemble elasto-plastic behavior. However, rotation of the beams forced some bolts in the friction devices to bear against the sides of the slotted holes, and resulted in the post-slip stiffness that is evident in the story shear versus drift plot. Demand on many of the components used in the connection (such as the failed weld between plates) exceeded design capacities as a result. The assemblage of plates used in the top connections and the high-strength bolts used in the bottom connections introduced connection flexibility at low drift levels that was approximately twice that observed for the other specimens. Designers

should be aware that the overall flexibility of precast beam-column connections is very sensitive to the stiffness of the connecting elements, and as result, proportions of connections between precast elements can be controlled by stiffness rather than strength.

Nonlinear Elastic Concept

UMn-PTS/PTB were two specimens that represented the nonlinear-elastic post-tensioning concept (5). The precast beams and columns were connected with unbonded post-tensioning steel which passed through the joint and was anchored in horizontal "dogbones" located at the beam ends (Figs. 17 and 18). The intersecting spiral reinforcement shown in the top and bottom regions of the beam dogbones was provided to enhance the concrete confinement in those zones.

The difference between specimens UMn-PTS and UMn-PTB consisted in member sizes and post-tensioning types: UMn-PTS used monostrands (multistrands in the prototype), and UMn-PTB had shallower beams and used high strength threaded bars. The beams were deeper in the case of PTS to accommodate the strand anchoring plates. The monostrand/multistrand system offers more economical use of post-tensioning steel while the threadbar is more easily installed and exhibits less significant seating losses than the former.

To achieve nonlinear-elastic behavior, the connection post-tensioning steel should remain elastic even when subjected to large lateral deformation levels. The choice of the initial prestress is critical to guarantee this kind of behavior (5). The initial prestress was limited to the amount required to ensure the beam-column interface joint would remain closed under the design gravity and wind loads. During seismic loading, the connection opens creating a concentrated beam rotation at the column interface. During this process it is intended that the post-tensioning steel not be stressed into the inelastic range. As a consequence, the connection returns to its undeformed position upon unloading. During this process the connection is able to accommodate relatively large deformations while maintaining its load carrying capacity. The nominal required moment capacities of the beams at the interface of the dogbone region were increased by 30 percent to insure that the deformations remained concentrated in the connection regions while the members themselves remained relatively undamaged.

Both specimens, UMn-PTS and UMn-PTB, performed quite well for design level drifts up to 3%. Figure 19 shows a plot of story shear versus drift for UMn-PTS. Figures 20 and 21 illustrate the moment versus rotation response with respect to the superimposed predicted

behavior for UMn-PTS and UMn-PTB, respectively. The moment refers to the moment at the beam-column interface. The measured rotation refers to the rotation of the beam relative to the column measured within 7 in. from the interface. Predicted rotations represent the concentrated rotations calculated from assumed crack openings at the column-dogbone interface.

The predicted behavior was obtained using the model proposed by Priestley and Tao (5) that was used to size and detail both connections. The relationship between load and displacement is assumed to be linear until the compression force in the outermost concrete fiber is zero; this point is defined as M_{cr}. The value of M_{cr} can be evaluated by force balance within the cross section. The value of the external force, F_{cr}, needed to generate that moment is found by geometric considerations. The behavior of the connection is further considered linear up to a moment of twice M_{cr}. At this moment, designated M_2, the crack opening is assumed to have propagated to the centroid of the section (the prestressing steel is assumed concentrated along the centroidal axis). The value of the corresponding external applied force is twice F_{cr}. After this point the behavior of the connection will start to deviate considerably from linear. For a point beyond this "linear" limit, the value of the moment was evaluated by internal force balance, as a function of the stress in the prestressing steel and an assumed equivalent rectangular concrete compression block. The change in steel stress at points above M_2 result directly from the crack opening at the assumed centroid of the prestressing steel. This elongation causes a concentrated rotation to develop in the connection region. This information can be used to determine the increased beam end rotations and drifts.

In reviewing Fig. 20, it can be observed that the prediction gave a reasonably close envelope curve for the experimental data. The sensitivity of the model to the assumed concrete spalling depth is apparent in the plots where the expected behavior of the specimens is presented both for an assumed spalling depth of 0.75 in., equal to the depth of the concrete cover, and for an assumed spalling depth of 1.5 in., equal to the average depth of the concrete not confined by the dogbone spiral reinforcement. Even though extensive spalling was not observed on a large scale during the tests, deterioration of the grout joint and the consequent increase in the relative rotation between beams and column, make the assumption of a spalling depth of 1.5 in. reasonable.

Connection PTS was taken to drifts exceeding 3% while exhibiting stable hysteretic behavior; the peak story shear was reached during the first cycle at 3% drift. In the next set of cycles to 4% drift, the story

shear necessary to reach that drift was lower than the maximum story shear attained during the previous set of cycles to 3%. Due to failure of the strain gages during the post-tensioning operation for specimen PTS (as a consequence of damaging the gages during strand installation) it was not possible to investigate the behavior of the post-tensioning steel during testing to determine at which drift level yielding of the strands initiated. When the specimen was initially displaced to 3% drift the monostrands started to fracture (this was assumed after hearing a loud snapping noise and observing the simultaneous dropping of the load necessary to maintain the specimen at that drift level). The fracture of more strands in the following cycles to 4, 5, 6, and 7% drift levels impaired the clamping action of the post-tensioning strands; this can be seen in the story shear-drift plot where substantial pinching was observed during load reversal. It is important to notice that fracture of the strands occurred at drift levels higher than 3%; at those drift levels elongations of the strands were such that stresses in the steel were well beyond the yield point. During tension tests performed on the post-tensioning steel, the strands did not show much capacity after yielding, therefore the failure of the strands was not considered premature.

Connection PTB was taken to drifts exceeding 4% while exhibiting stable hysteretic behavior; it was only at the first cycle to 5% drift that the peak load necessary to reach that drift was lower than the peak load attained in the previous set of cycles to 4% drift. The moment-rotation plot (Fig. 21) showed little evidence of pinching at low values of moment during the load reversal phases; an indication that no significant loss of the post-tensioning clamping force took place. A story shear-drift plot is not presented for this specimen because movement of the loading frame during testing contaminated the drift data. Data obtained from strain gages mounted on the post-tensioning bars in PTB showed that there was indeed no yielding of the post-tensioning steel up to the design moment. Yielding of the bars started to occur at drift levels of approximately 4%. Spalling of the concrete cover in the dogbone side areas and consequent reduced bearing support under the post-tensioning bar anchor plates initiated at 4% drift and continued until the extent of damage was such that the post-tensioning bars deformed out of plane and the test was considered concluded. This failure was observed at a value in excess of 9% drift while loading monotonically from 6 to 10% drift.

The behavior of both connections was close to nonlinear elastic up to the design drift level. It was only in the final part of each test, when the specimens were taken to failure, that the areas within the hysteresis loops began to increase as a consequence of concrete cracking and yielding of the steel reinforcement (both conventional and

post-tensioning). As mentioned earlier, this inelastic behavior can be considered as a positive phenomenon when energy dissipation is taken into consideration. From the moment-rotation response for PTS (Fig. 20), it can be seen that in the final part of the test, at load levels beyond the design moment of 317 ft-k, rupture of the post-tensioning strands caused severe pinching of the hysteresis loops.

UT-PTS was the third connection tested that was intended to investigate nonlinear-elastic behavior. This connection differed from the connections tested at the University of Minnesota in that the precast beam was continuous through the connection region (see Fig. 22), and the beam was pretensioned instead of post-tensioned. The prototype system from which this specimen was derived was envisaged to have precast beam elements that spanned from midspan to midspan over two columns. Beams would be connected at midspan to resist shear and gravity moments only. Precast column elements would span between floors.

Specimen UT-PTS was pretensioned using 20 centrally-located 3/8 in. diameter strands pretensioned to 40% of f_{pu}. In order for the strands to remain elastic through specimen drifts of 2%, they were debonded through the joint and for 2 ft. on each side of the column (a total of 69 in.). Spiral reinforcement was placed in the top and bottom of each beam within 18 in. from the column interface to confine the concrete and permit large rotations at the beam-column interface. Approximately 75% of the joint reinforcement recommended by ACI-ASCE 352 (10) was used in the specimen. This was done with the hope of precipitating a joint failure because none of the other specimens exhibited signs of significant distress in the joint region, and because the force transfer mechanism for joints in prestressed specimens (with unbonded prestressing through the connection) is comprised primarily of a direct compression strut (a mechanism which differs substantially from behavior of monolithic joints at low load levels).

Specimen UT-PTS was assembled by first placing the lower column segment into the test setup. The beam/joint segment was then lowered over the 16 column bars that protruded from the top of the lower column segment. The half inch gap that was left between the lower column segment and the beam/joint segment was grouted along with the ducts in the beam/joint segment. The upper column segment was lowered into position and column bars were joined immediately above the beam using threaded couplers. The recess provided around the base of the upper column segment to accommodate the threaded couplers was filled with fiber reinforced grout.

Story shear versus drift response for the specimen is shown in Fig. 23.

Behavior through the 2% drift cycles generally resembled measured behavior of UMn-PTS (Fig. 19), except hysteresis loops for UT-PTS were pinched at low drift levels. Pinching was the result of slip in the column bar couplers once the column cracked. The pinching would have been substantially less if axial load had been applied to the column (no axial load was applied to any of the columns) and if commercial products intended for coupling conventional bars had been used. Commercial bar couplers were not used because of the extreme congestion that existed in the half-scale specimen.

Energy dissipation increased markedly during the cycles to 4% drift, but not as the result of yielding of strands. Strain gages mounted on strands in the debonded regions indicated that strands remained elastic throughout the test. It was presumed that bond between the concrete and strand deteriorated outside the debonded region (increasing the debonded length) as the test progressed. The substantial increase in energy dissipation was attributed to failure of the joint. Although transverse reinforcement began yielding at approximately 1.5% drift, significant dilation of the joint and obvious crushing of concrete along diagonals of the joint were not evident until cycles to 4% drift. Even though concrete spalling adjacent to the column face was as much as 1 in. during cycles to 5% drift (only slightly more than the cover thickness), it is believed that deterioration in connection strength was primarily the result of damage incurred by the joint.

COMPARISON OF SPECIMEN RESPONSE

In the interest of brevity, comparisons of specimen behavior, based on the observations contained in the discussions of individual specimen response, will be made in the summary section. The following discussion focuses on stiffness degradation and residual drifts observed during the tests.

Stiffness Comparisons

Small amplitude intermediate displacement cycles (to loads representing 75% of the previously attained peak loads) were used to provide information about stiffness degradation in the specimens. Intermediate displacement cycles were not applied until drifts reached 0.25%. For displacement cycles below 0.25% drift, data from the peak response in each cycle was used. Stiffness values for each of these cycles were calculated using the story drift (equivalent column displacement) at zero load and the story shear and drift at peak response (i.e. secant stiffness). Stiffnesses were calculated for both positive and negative loading cycles.

Figure 24 presents secant stiffnesses for all test specimens as a function of the maximum drift level attained during the previous displacement cycles. For drifts less than 0.25%, stiffness was plotted versus actual drift. Stiffnesses for UMn-PTB corresponded with drift cycles administered after instrumentation was installed to monitor movement of the loading frame.

The most significant stiffness reduction for all specimens occurred during the initial displacement cycles, and was primarily due to member cracking. Initial stiffness values varied by as much as 75% (UMn-PTS vs. UMn-GAP). Some differences in initial stiffness can be explained because of differences in member proportions or connection details. For instance, the column in UMn-PTB was larger than that used in most of the other specimens, and the depth of beams in UT-DB was reduced by 25% over much of the beam length. Furthermore, UT-FR incorporated a complicated plate assembly for the top connection between the beams and column and high-strength bolts for the bottom connection that introduced additional flexibility in the specimen.

The trend in stiffness degradation was similar for all specimens, although specimens having the highest initial stiffness tended to experience a higher rate of degradation. This is illustrated in Fig. 25 by normalizing the secant stiffness data presented in Fig. 24 by the maximum secant stiffness for each specimen. Note that specimens with the highest initial secant stiffness in Fig. 24 typically had the lowest normalized stiffness in Fig. 25 for drifts of 0.75% or larger. It should be noted that two of the specimens, UMn-TCY and UT-GAP, demonstrated significant amounts of pinching in the story shear - drift responses at drifts as low as 1%. Stiffness degradation was substantially higher for these specimens considering the tangent stiffnesses (computed at low load levels).

Residual Deformations

To investigate the ability of each connection to return to its original undeformed position following unloading, the residual displacement after each set of cycles was evaluated. Results are given in Fig. 26 as a function of the maximum drift level reached during the previous set of cycles. Residual deformations were evaluated with respect to the original undeformed position at the beginning of each test. The plot can be divided in three regions. The first region, from the start of the test up to an applied drift of 1% shows relatively minor differences in residual drifts for all specimens. Most of these differences can be attributed to slip in the connection details that utilized indirect load transfer paths.

In the second region, between 1 and 3% drift levels, prestressed connections exhibited slight increases in residual drifts that remained between 0.1% (UMn-PTS) and 0.3% (UT-PTS), while the residual drifts for the other connections reached 1% or more. This difference reflects anticipated differences in behavior between the three connection concepts. The nonlinear elastic connections (UMn-PTS and PTB, and UT-PTS) can undergo relatively large deformations without sustaining significant permanent deformations. After unloading, the connections can return to a configuration close to the original undeformed one. Specimens tested to study the tension-compression yielding concept (UT-GAP and DB, and UMn-GAP and TCY) are supposed to deform plastically in tension and compression as a means to dissipate energy through hysteresis. Consequently, these specimens developed permanent deformations evident in Fig. 26. The sharp increases in residual drift values can be seen as a consequence of the many factors that finally led to specimen failure: yielding and elongation of beam longitudinal reinforcement for UMn-GAP; yielding and elongation of longitudinal reinforcement with related sliding of the beams with respect to the column, slip of corrugated pipes within the column due to deteriorated bond, and buckling of longitudinal beam reinforcement for UMn-TCY; and yielding and elongation of beam longitudinal reinforcement combined with inelastic flexural and shear deformations in vertical bars at the interface between beams and corbels for UT-GAP. The specimen tested to examine the influence of an energy dissipating device in a connection (UT-FR) was also supposed to deform "plastically" to dissipate energy. The "permanent" deformations that developed in this specimen as the result of friction plates sliding past each other were greater than for the other connections. These deformations could be relieved by loosening the bolts in the friction connection device and restoring the connection to its original undeformed position.

In the third region, where applied drift levels are higher than 3%, an increase in residual drift was observed for all specimens (test data for specimens UT-DB, UMn-GAP, and UT-GAP did not exist for drifts greater than 3%). In the case of UMn-PTB and PTS the increase in residual drift was primarily due to yielding of the post-tensioning bars and rupture of some post-tensioning strands, respectively. For UT-PTS, the increase was related to deterioration of the joint region. Strands in this specimen did not yield. For UMn-TCY the increase was due to the aforementioned deformation process and the resulting specimen degradation. It is important to notice that the magnitude of the final residual drifts was substantially different for the two types of connection concepts: at an applied drift level of 4%, the residual drifts for UMn-PTB, UMn-PTS and UT-PTS were on the order of 0.5%, while for UMn-TCY it was approximately 1.6%.

ANALYTICAL MODELING OF PRECAST SYSTEMS

The subassemblage tests provided detailed information about the behavior of individual connections, particularly in the form of load-deformation hysteretic response. This information was incorporated into nonlinear dynamic analyses of five- and fifteen-story frame systems subjected to a variety of ground motions. The analyses were conducted using the DRAIN-2DX program developed in PRESSS Phase I. The objective of the analyses was to establish gross measures of response, such as story drifts, global and local ductility demands, etc., necessary to determine the suitability of the frame systems incorporating the various connection details in seismic regions. The results were compared with those of an idealized cast-in-place structure.

The fifteen-story frame system that is being analyzed is one of the perimeter frames of the structure described earlier (Fig. 2) which was designed by Englekirk and Sabol Consulting Engineers, Inc. The five-story frame structure had the same footprint as the fifteen-story building and was proportioned in a manner consistent with the design of its larger counterpart; using the equivalent lateral force procedure in the UBC for Seismic Zone 4, an R_w of 12 and S equal to 1.2.

Two of the hysteretic models used are shown in Figs. 27 and 28: a nonlinear inelastic model and a nonlinear elastic model. These models are idealized to represent the behavior of monolithic reinforced concrete and precast prestressed concrete connections, respectively. The nonlinear inelastic model is currently available in the DRAIN-2DX program; the stiffness degrading model is one of two developed at the University of Minnesota to characterize the behavior of the nonlinear-elastic precast connections observed during the laboratory tests. The model introduces distinct bilinear loading and unloading lines. After unloading occurs, the next loading takes place along the previously defined unloading branch. The slopes of the unloading branches depend on the maximum deformation level reached at the onset of unloading.

The computed roof-level displacement responses for the five and fifteen-story frames with the hysteretic models shown in Figs. 27 and 28 and subjected to the 1940 El Centro NS acceleration record (scaled to a peak acceleration of 0.4g) are shown in Figs. 29 and 30. Maximum displacements of the frame systems with "prestressed" connections exceeded displacements for the "monolithic" systems by 50 and 75% for the five and fifteen story frames, respectively. The calculated displacement waveforms for the precast prestressed frames exhibited slightly longer apparent periods than the waveforms for the

monolithic frames. The most noticeable difference between the two systems is in the magnitude of the residual displacements. At the end of the seismic disturbance, the "prestressed" connections exhibited negligible residual displacements for both the five and fifteen story buildings, while the "monolithic" buildings were left with roof eccentricities of approximately 0.8 and 2.5 in., respectively.

SUMMARY

Research has been conducted to investigate the behavior of ductile moment-resisting connections between precast beam and column elements. The connections evaluated may be classified into three behavioral categories: tension-compression yielding, energy-dissipating, and nonlinear-elastic. Eight connections from these categories were subjected to reversed cyclic load tests to characterize their behavior. Results of the tests were used to develop analytical models incorporating the observed connection behavior to investigate the suitability of details tested in this program for seismic regions and to develop recommendations for the design of ductile beam-column connections.

All of the specimens, except UT-DB and UMn-GAP, performed well through design-level drifts. Specimen UMn-GAP experienced bar fractures at the face of the bar couplers during 2% drift cycles, and UT-DB experienced concrete crushing in the dogbone regions of the beams as a result of using a connection detail that incorporated an indirect path for transfer of forces at the ends of the beams. This same problem (indirect force path in the connection region) contributed to failure of UT-GAP (fracture of dowel bars in bottom connection between beams and corbel) and UT-FR (fracture of a weld in the energy-dissipating connection) during 3% drift cycles. The indirect force path inherent in the connections also resulted in additional flexibility that was most apparent at low drift levels. Particular attention must be paid to designing these connections for appropriate levels of stiffness.

Although not all specimens performed as well as others, most contained at least one connection detail that demonstrated good performance throughout testing. For example, the corbel/dapped beam combination used in UT-FR and the lightly post-tensioned bars used in the bottom of beams in UMn-GAP did not deteriorate during testing, and they provided a well-defined "pivot point" to accommodate deformations developed in the connections at the beam tops. Note that these gap connections could also be inverted, providing the gap at the beam bottom to avoid distortion and damage in the slab/horizontal diaphragm. Care must be exercised, however, in choosing the other

connection to be paired with these connections. Specimen UMn-GAP apparently failed because of the severe inelastic demand that was placed on the coupled bars in the top of the beams.

Prestressed specimens, UMn-PTB and UT-PTS, exhibited the desired nonlinear elastic behavior through 3% drift levels, while UMn-PTS apparently experienced strand fractures during load cycles to the same drift level. All of the unbonded prestressed specimens experienced minimal residual drifts during cycles up through design drift levels. Energy dissipation for these connections was quite low for the same drift levels. In contrast, energy dissipation for the connection containing a friction device (UT-FR) was quite high. The higher cost associated with the friction connection may preclude the use of such a connection throughout the structure, but the superior energy dissipating characteristics suggest that a few of these connections placed at strategic locations in a structure, such as one utilizing prestressed connections, may dramatically improve the overall seismic resistance of the structure.

All but one of the connections tested in this study contained transverse reinforcement in the joint that was quite similar to that recommended by ACI-ASCE 352 (10). None of these connections demonstrated signs of joint distress, indicating that the ACI-ASCE 352 provisions are conservative for the design of most precast beam-column joints. Specimen UT-PTS was constructed with 75% of the joint reinforcement recommended by Committee 352. The specimen maintained strength and showed no signs of distress until the second drift cycle to 4%. More attention will be directed in the future to development of a design procedure for joint reinforcement in prestressed connections.

Analyses have indicated that precast prestressed frame systems may experience moderate increases in displacements as compared with monolithic concrete frame systems. The increased displacements appear to be less for larger period (fifteen-story vs. five-story) structures. The analyses verified reduced residual drifts associated with the nonlinear-elastic connection systems.

ACKNOWLEDGEMENTS

This research was carried out through the U.S. PRESSS program which is supported financially by the National Science Foundation, the Precast/Prestressed Concrete Institute, and the Precast Concrete Manufacturers Association of California. The views expressed herein are those of the authors and do not necessarily reflect the views of the sponsors.

BIBLIOGRAPHY

1. International Conference of Building Officials, Uniform Building Code, 1994 Edition, Whittier, CA, 1994.
2. Kurose, Y., Nagamai, K., and Saito, Y., "Beam-Column Joints in Precast Concrete Construction in Japan," American Concrete Institute Special Publication, SP-123, 1991, pp. 493-514.
3. Blakeley, R.W.G., and Park, R., "Seismic Resistance of Prestressed Concrete Beam-Column Assemblies," ACI Journal, Vol. 68, No. 9, Sep. 1971, pp. 677-692.
4. Blakeley, R.W.G., and Park, R., "Prestressed Concrete Sections with Cyclic Flexure," ASCE, Journal of Structural Engineering, Vol. 99, No. ST8, Aug. 1973, pp. 1717-1742.
5. Priestley, M.J.N., and Tao, J.R., "The Seismic Response of Precast-Prestressed Frames with Partially Debonded Tendons," PCI Journal, Vol. 38, No. 1, Jan./Feb. 1993, pp. 58-69.
6. Cheok, Geraldine S., and Lew, H.S., "Performance of 1/3-Scale Model Precast Concrete Beam-Column Connections Subjected to Cyclic Inelastic Loads," NISTIR 4433, NIST, Gaithersburg, MD, October 1990.
7. Cheok, Geraldine S., and Lew, H.S., "Performance of 1/3-Scale Model Precast Concrete Beam-Column Connections Subjected to Cyclic Inelastic Loads - Rep. No. 2," NISTIR 4589, NIST, Gaithersburg, MD, June 1991.
8. Popov, E.P., and Engelhardt, M.D., "Seismic Eccentrically Braced Frames," J. of Constructional Steel Research, Vol. 10, 1988, pp. 321-354.
9. Gregorian, C.E., Yang, T.S., and Popov, E.P., "Slotted Bolted Connection Energy Dissipators," Earthquake Engineering Research Center, Report No. UCB/EERC-92/10, July 1992, 21 pp.
10. ACI-ASCE Committee 352, "Recommendations for Design of Beam-Column Joints in Monolithic Reinforced Concrete Structures," ACI Journal, Vol. 82, No. 3, May-June 1985, pp. 266-283.

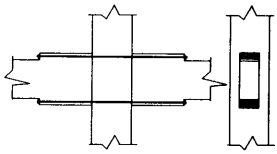

a) Vertical dogbones with threaded rebar

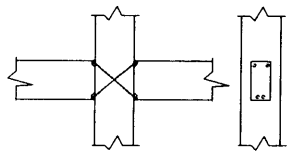

b) Cross-bars through joint

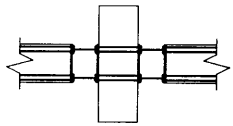

c) Steel beam detail

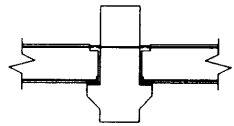

d) Welded detail

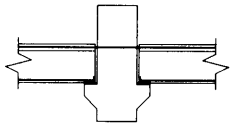

e) Gap joint

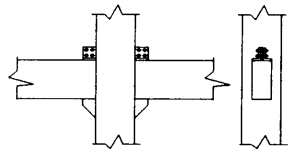

f) Friction plates

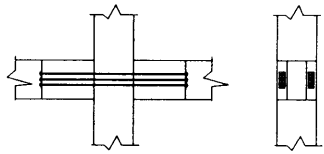

g) Horizontal dogbones with central post-tensioning

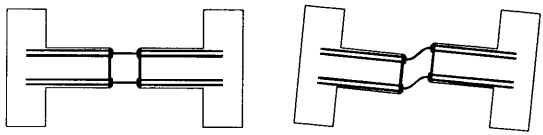

h) "Eccentric braced frame (EBF)" — Undeformed and deformed views

Fig. 1—Connection types considered in study

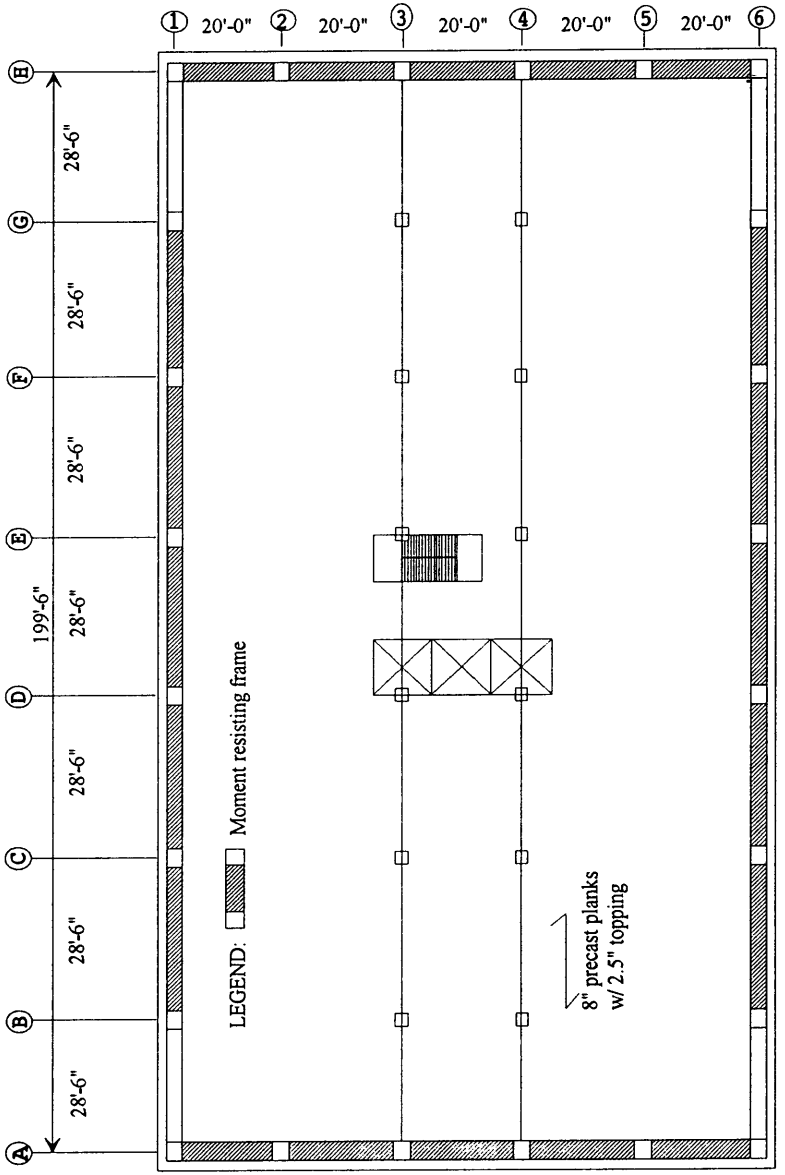

a) Typical floor plan

Fig. 2—Prototype precast frame building

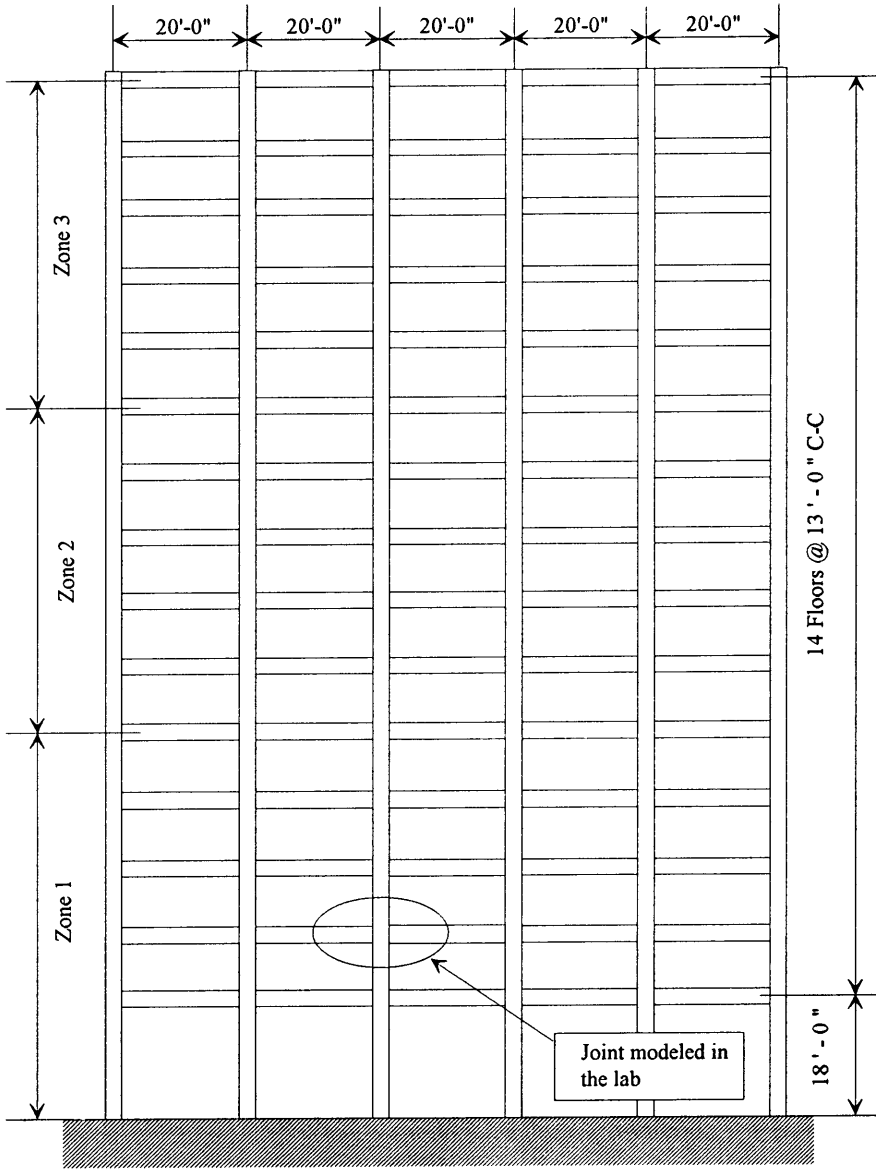

b) Elevation view

Fig. 2 cont.—Prototype precast frame building

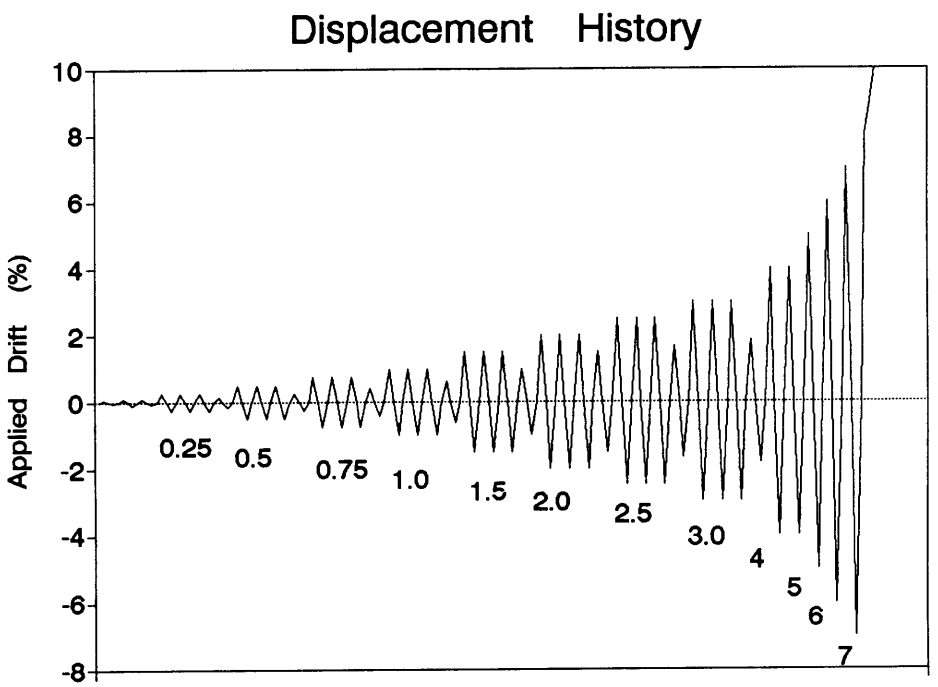

Fig. 3—Nominal displacement history

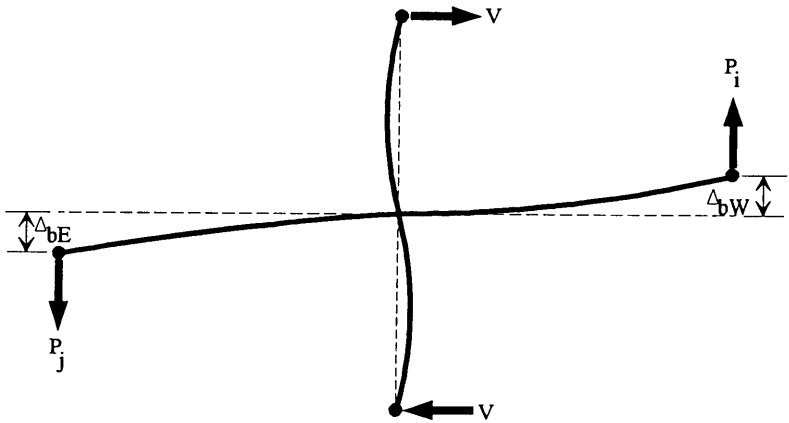

a) Deformed shape in test setup

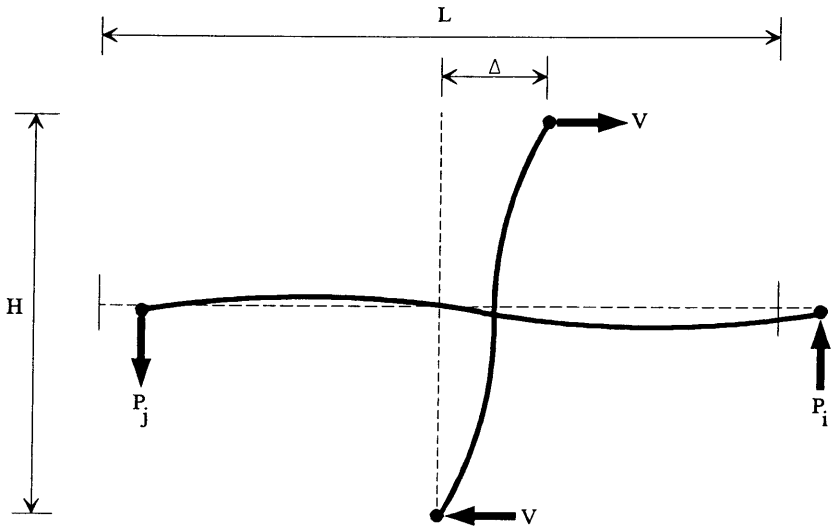

b) Ideal deformed shape for connection

Fig. 4—Deflected shape of subassemblages

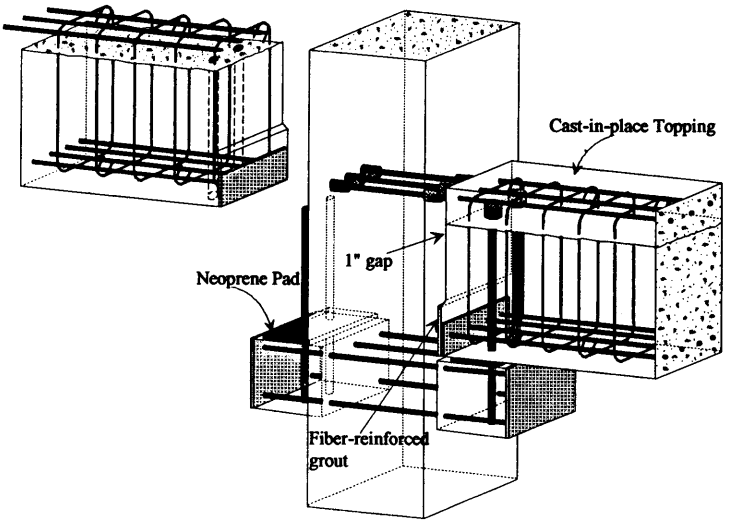

Fig. 5—Schematic of UT-GAP

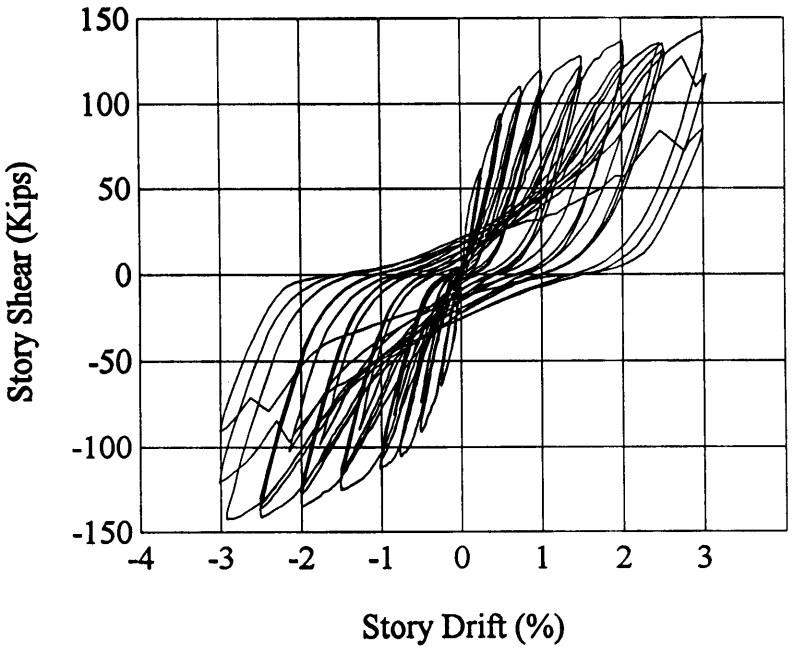

Fig. 6—Story shear-drift response for UT-GAP

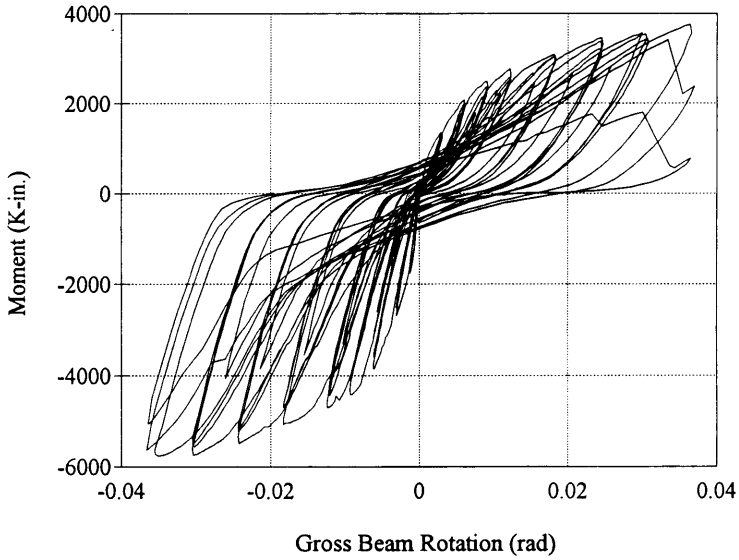

Fig. 7—Moment-rotation response for west beam of UT-GAP

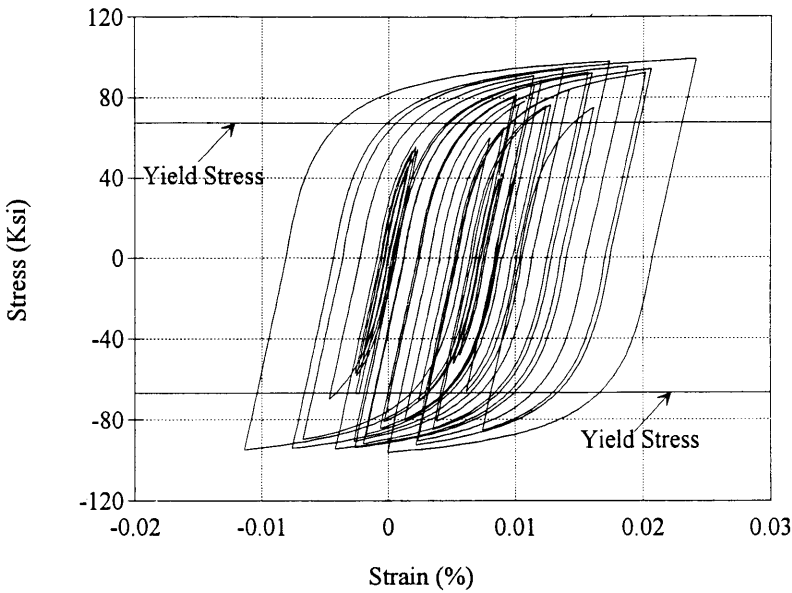

Fig. 8—Stress-strain response at column face for beam top bar in UT-GAP

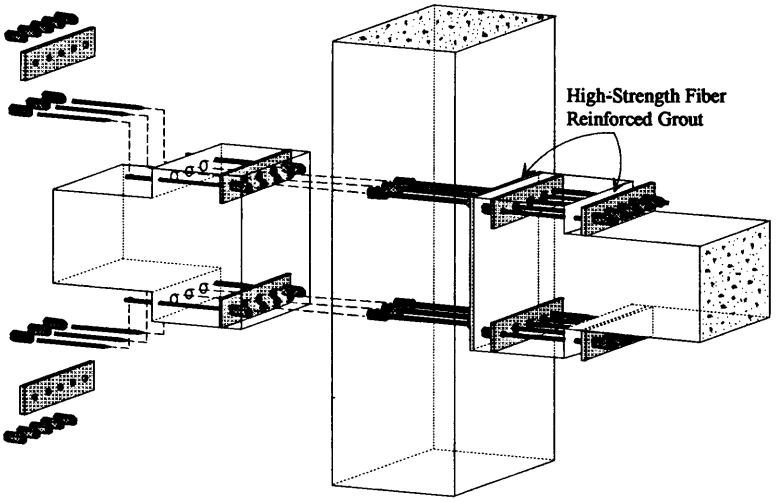

Fig. 9—Schematic of UT-DB

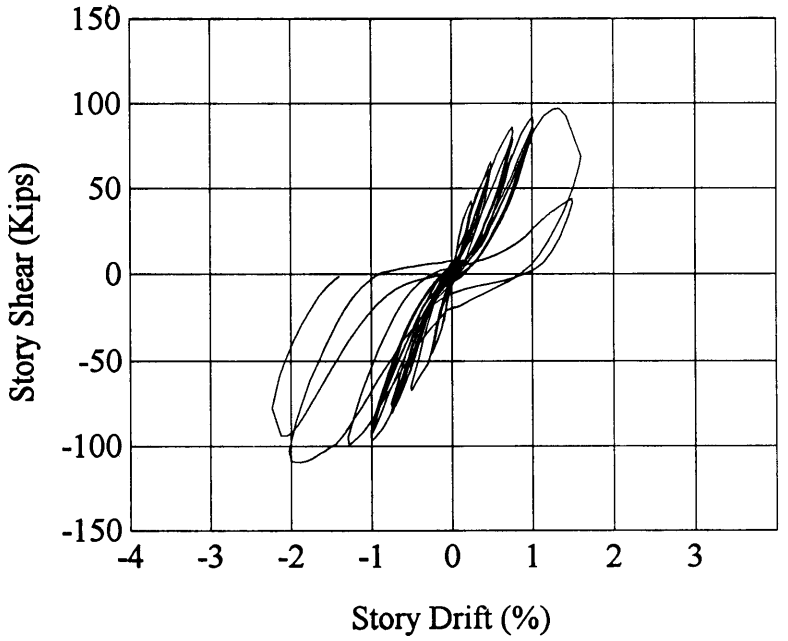

Fig. 10—Story shear-drift response for UT-DB

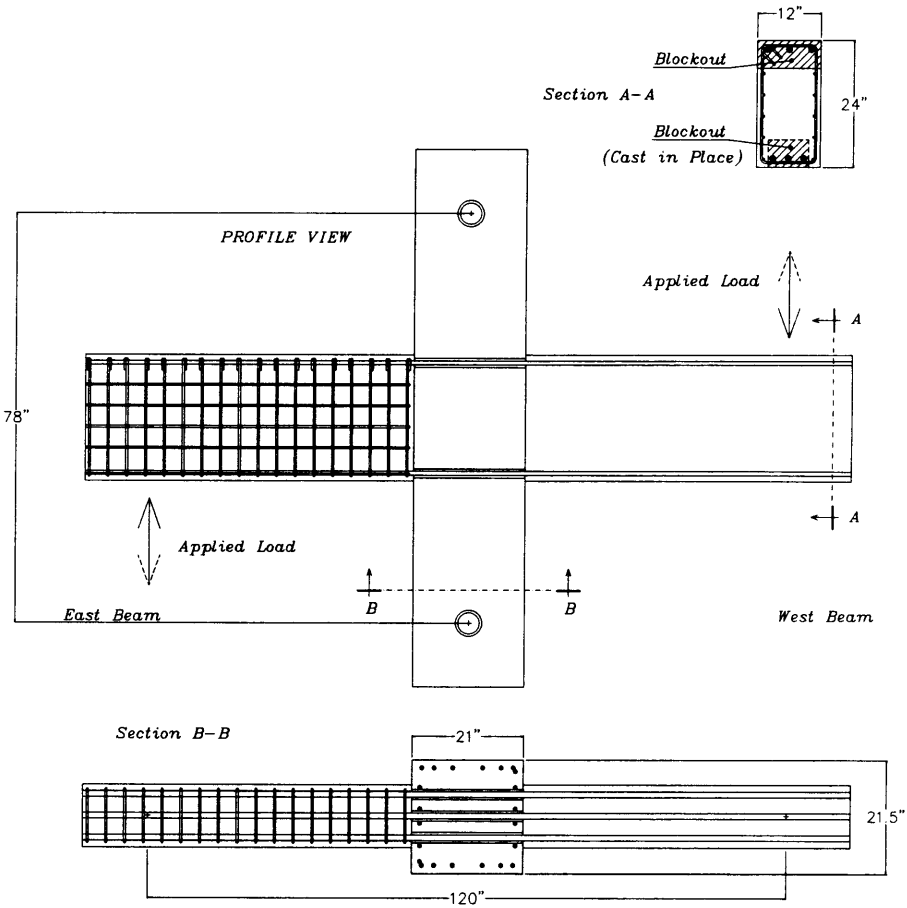

Fig. 11—Connection details for UMn-TCY

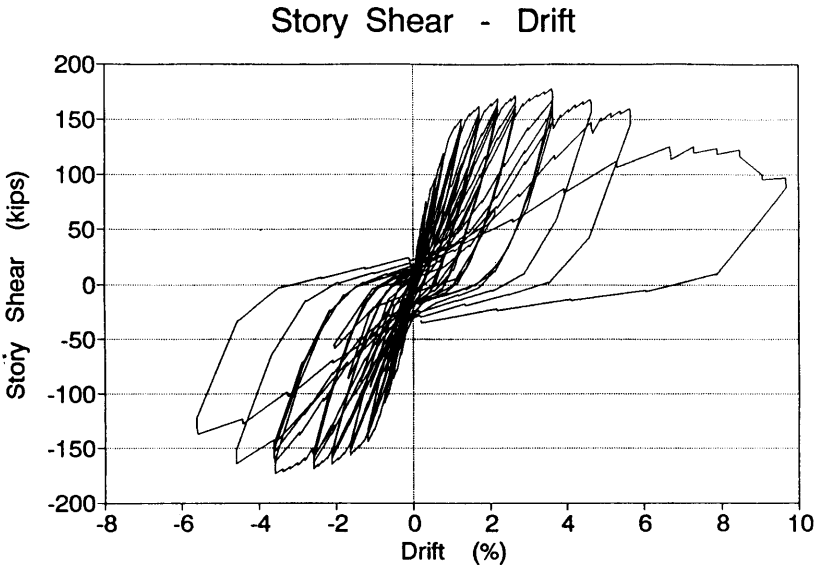

Fig. 12—Story shear-drift response for UMn-TCY

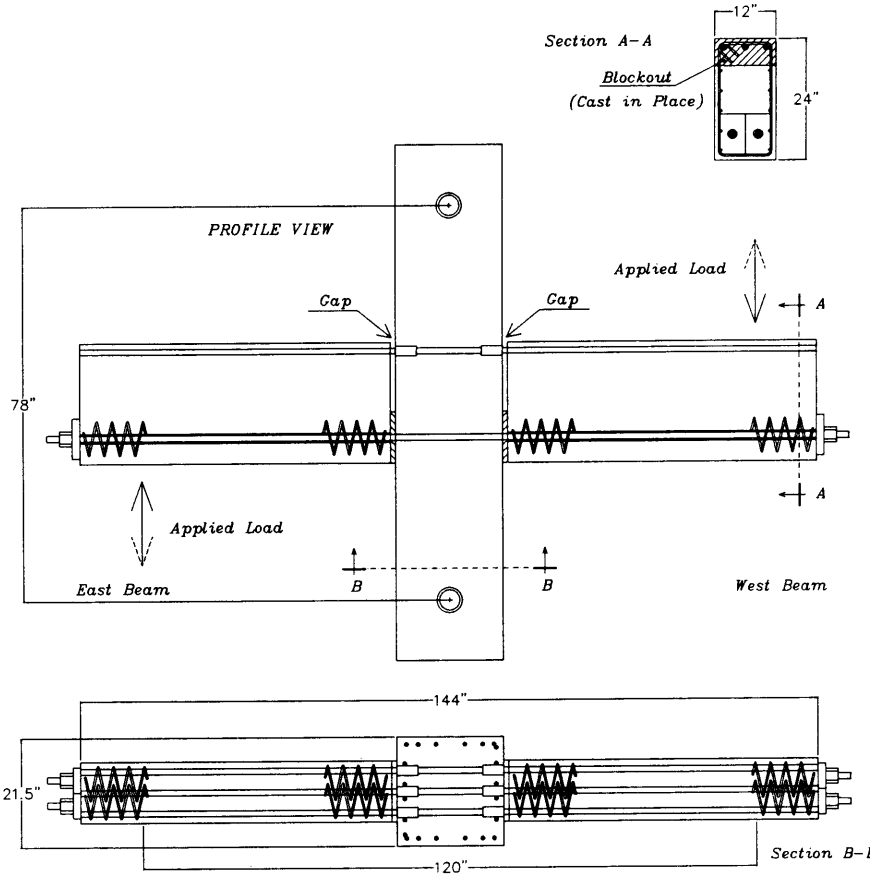

Fig. 13—Connection details for UMn-GAP

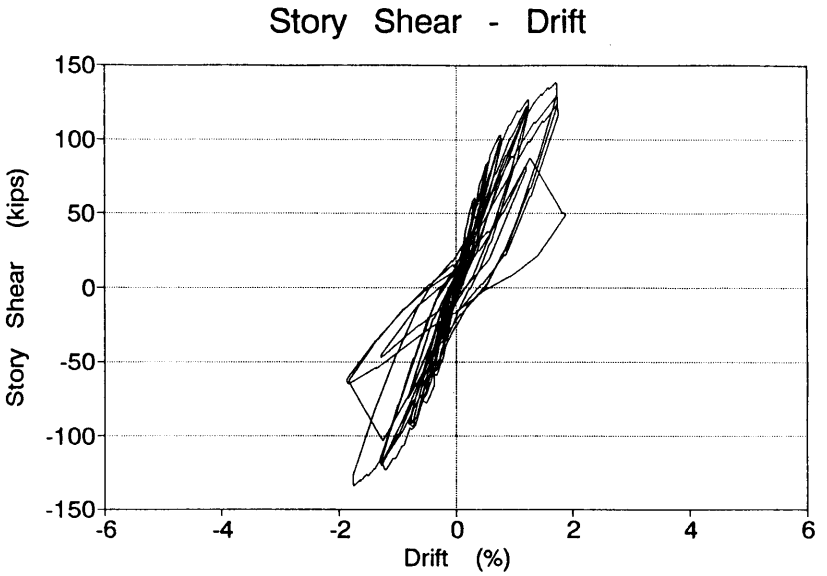

Fig. 14—Story shear-drift response for UMn-GAP

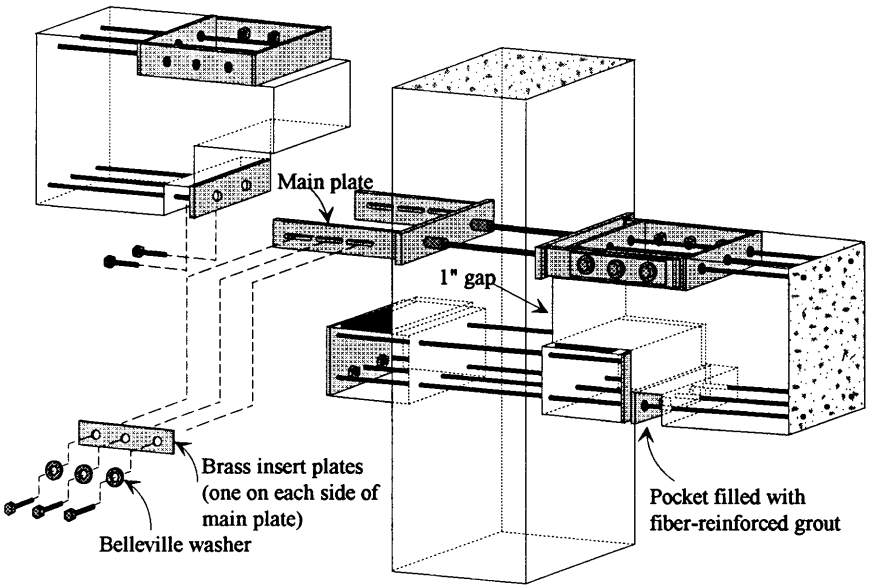

Fig. 15—Schematic of UT-FR

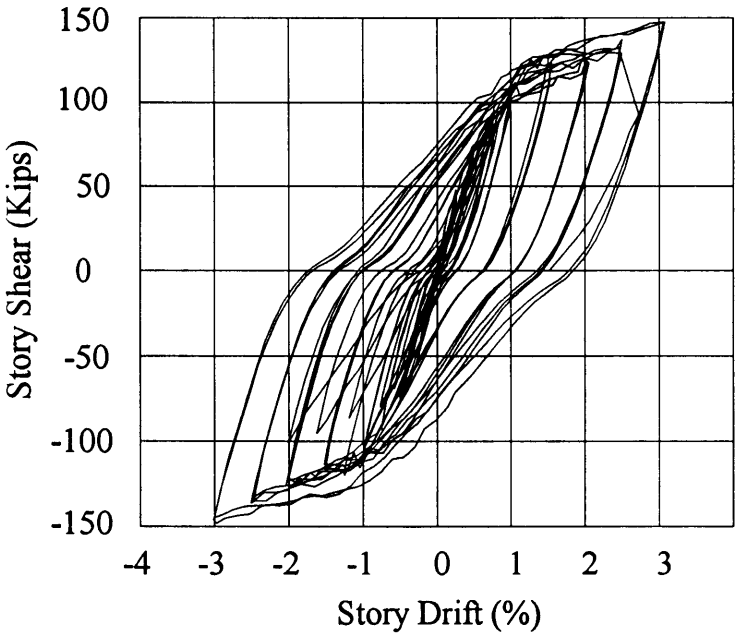

Fig. 16—Story shear-drift response for UT-FR

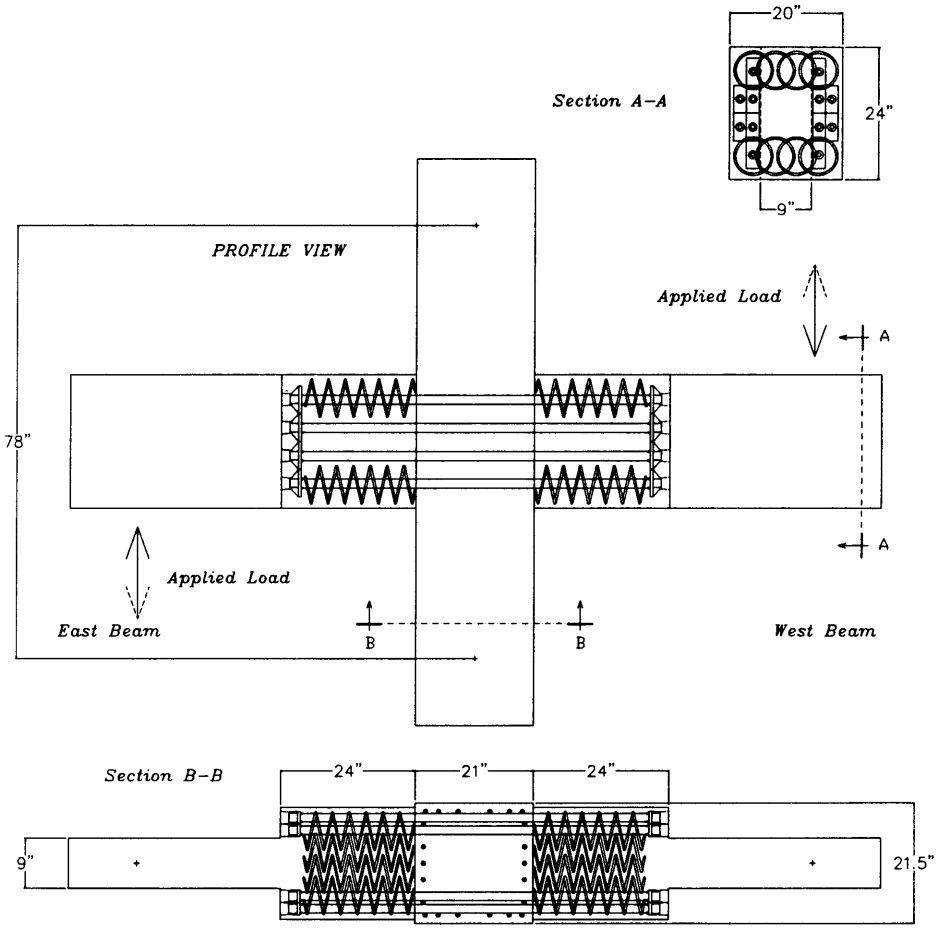

Fig. 17—Connection details for UMn-PTS

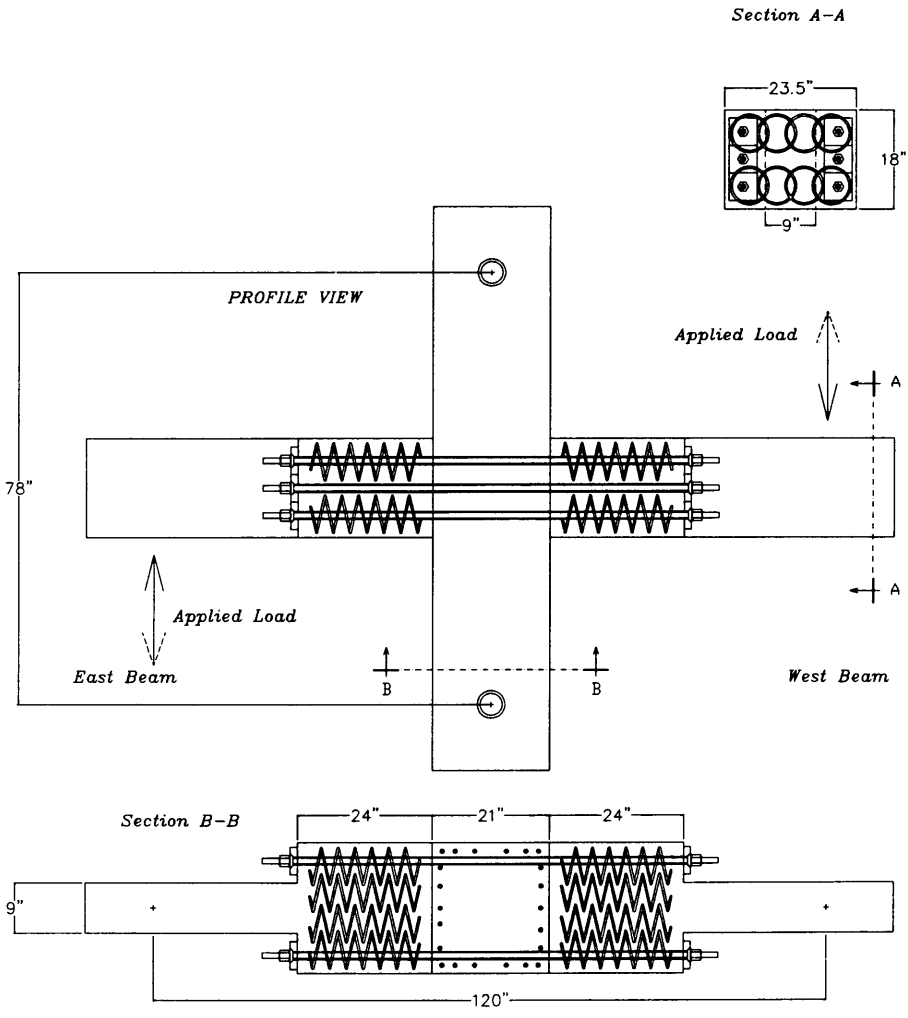

Fig. 18—Connection details for UMn-PTB

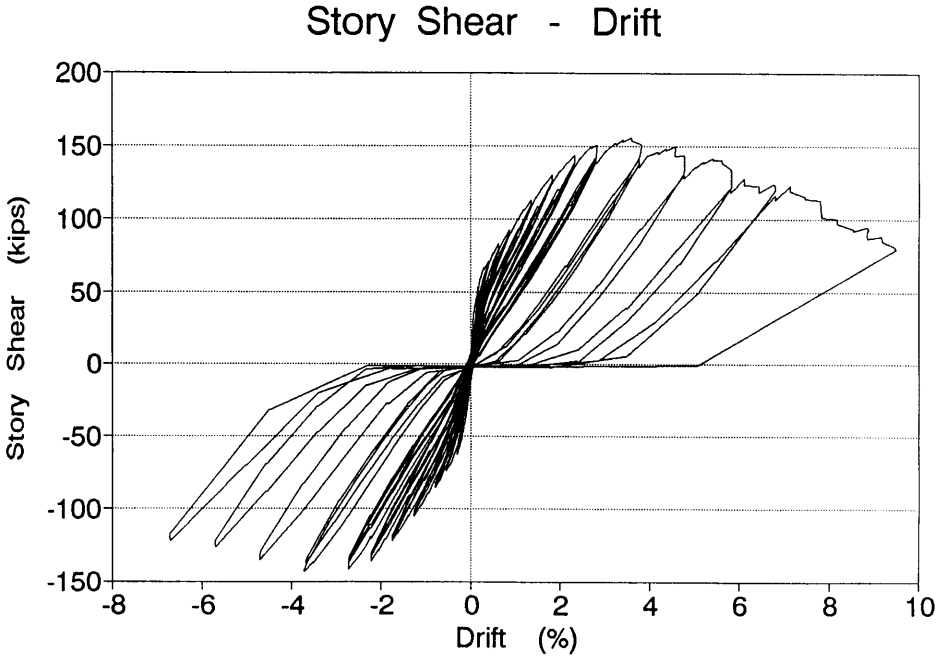

Fig. 19—Story shear-drift response for UMn-PTS

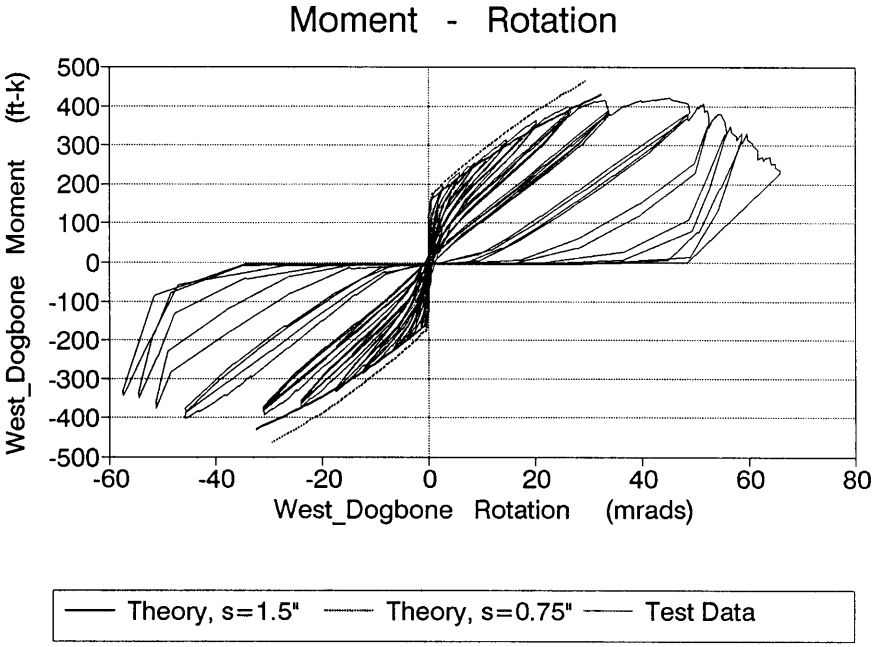

Fig. 20—Moment-rotation response for west beam of UMn-PTS

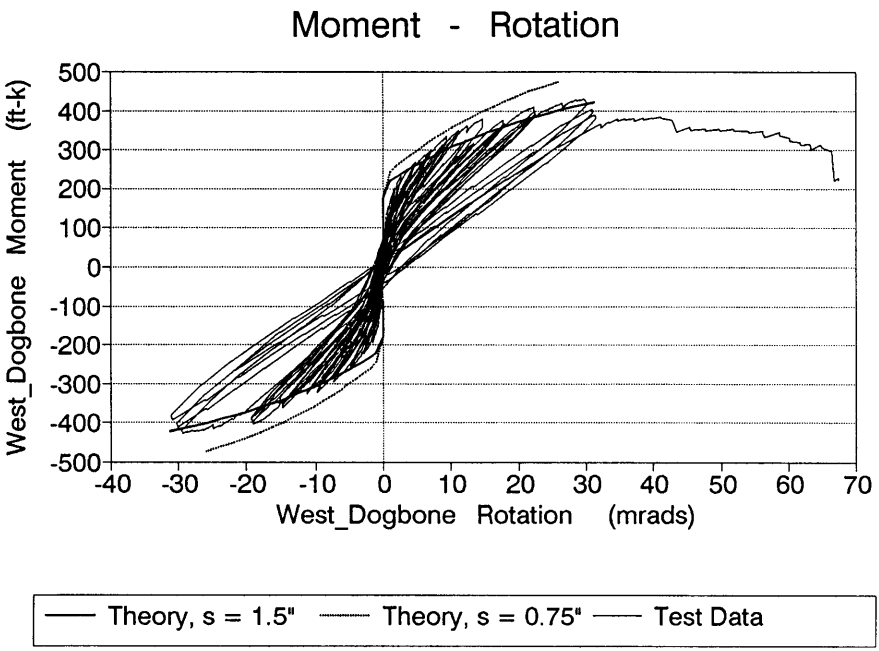

Fig. 21—Moment-rotation response for west beam of UMn-PTB

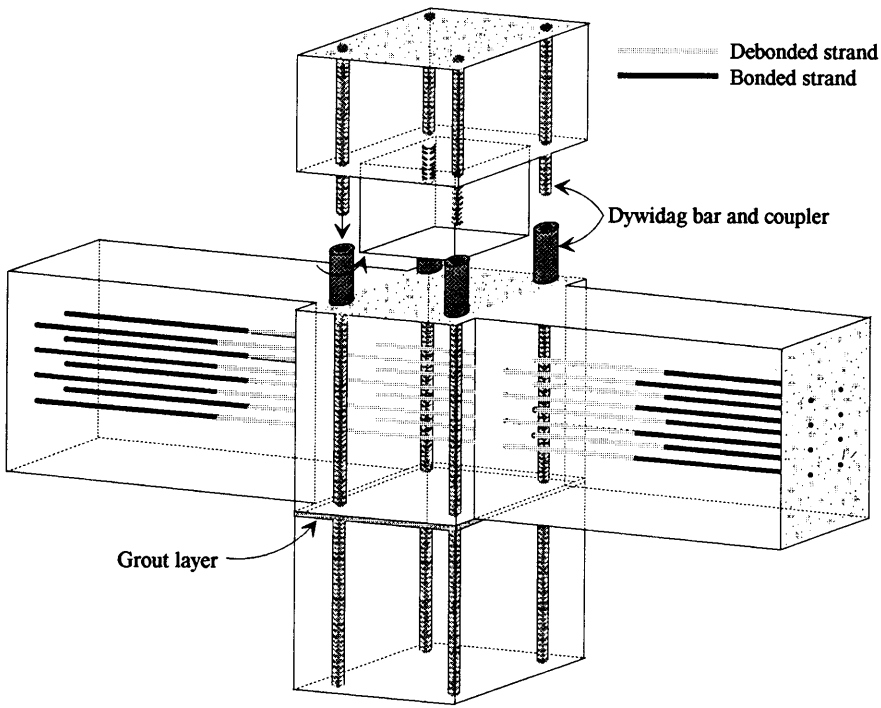

Fig. 22—Schematic of UT-PTS

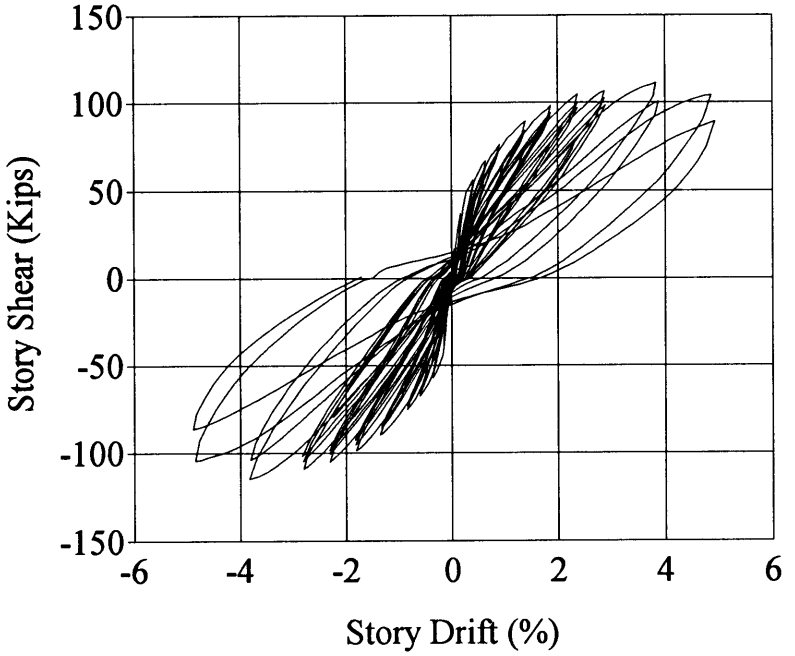

Fig. 23—Story shear-drift response for UT-PTS

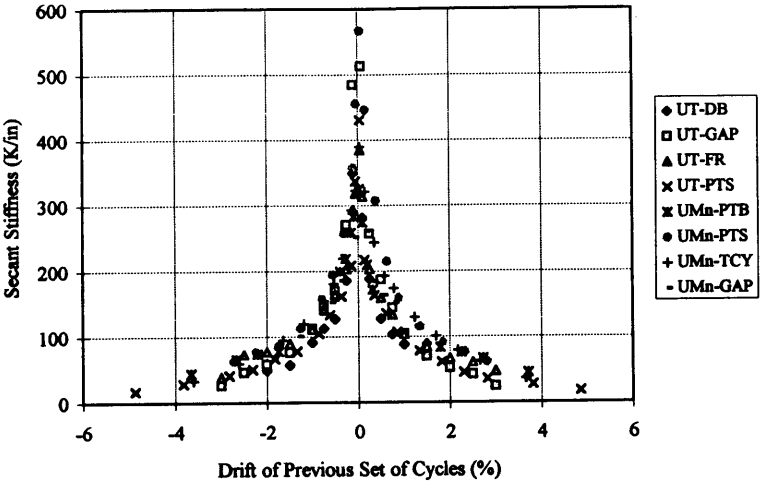

Fig. 24—Secant stiffness versus drift

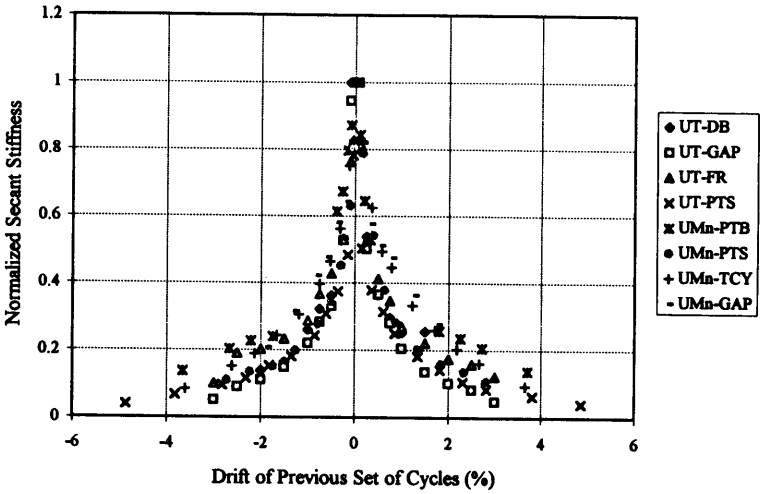

Fig. 25—Normalized secant stiffness versus drift

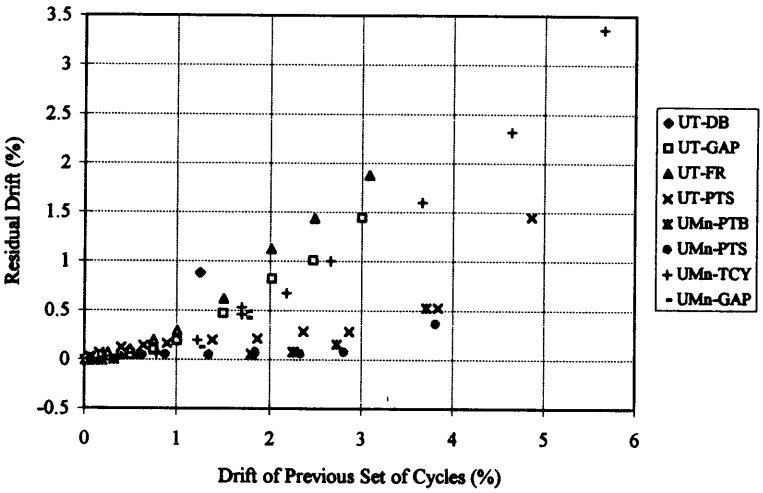

Fig. 26—Residual deformations for each set of drift cycles

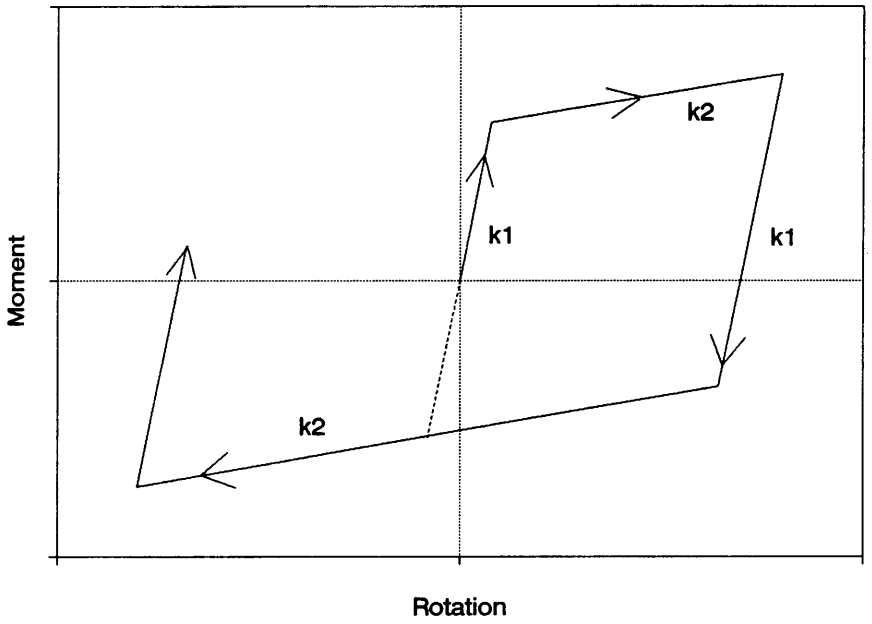

Fig. 27—Schematic on nonlinear inelastic hysteresis model

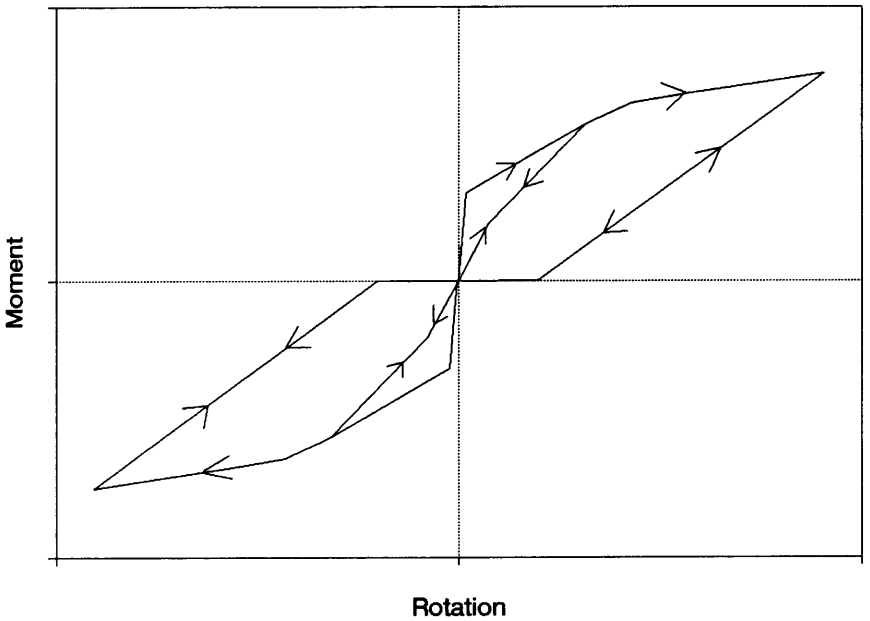

Fig. 28—Schematic of nonlinear elastic hysteresis model

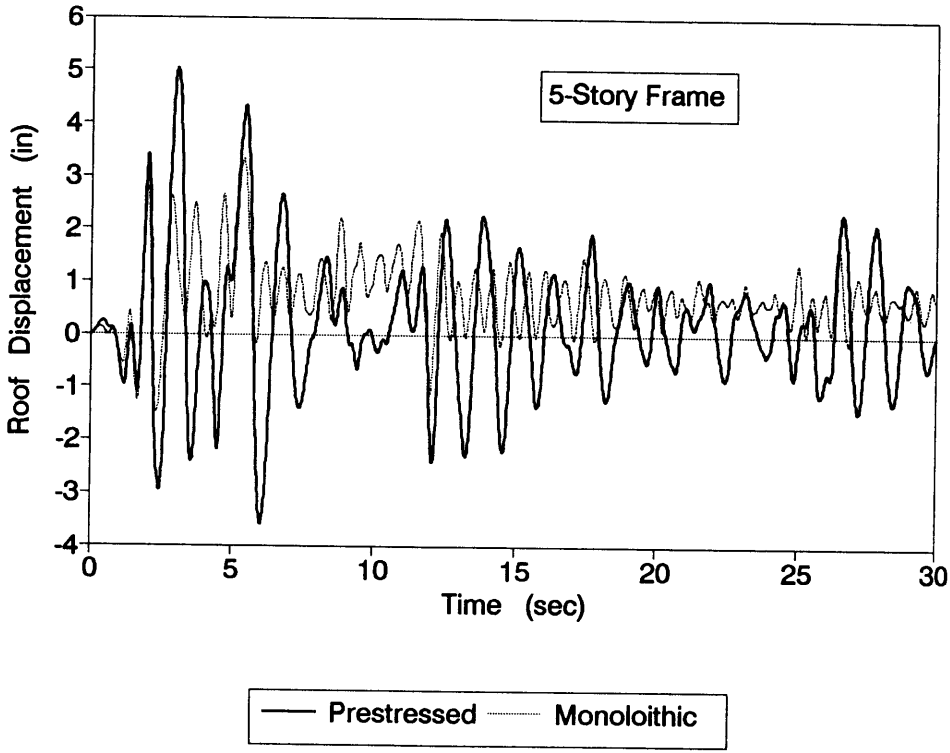

Fig. 29—Computed roof-level displacement response for five-story frame subjected to 1940 El Centro

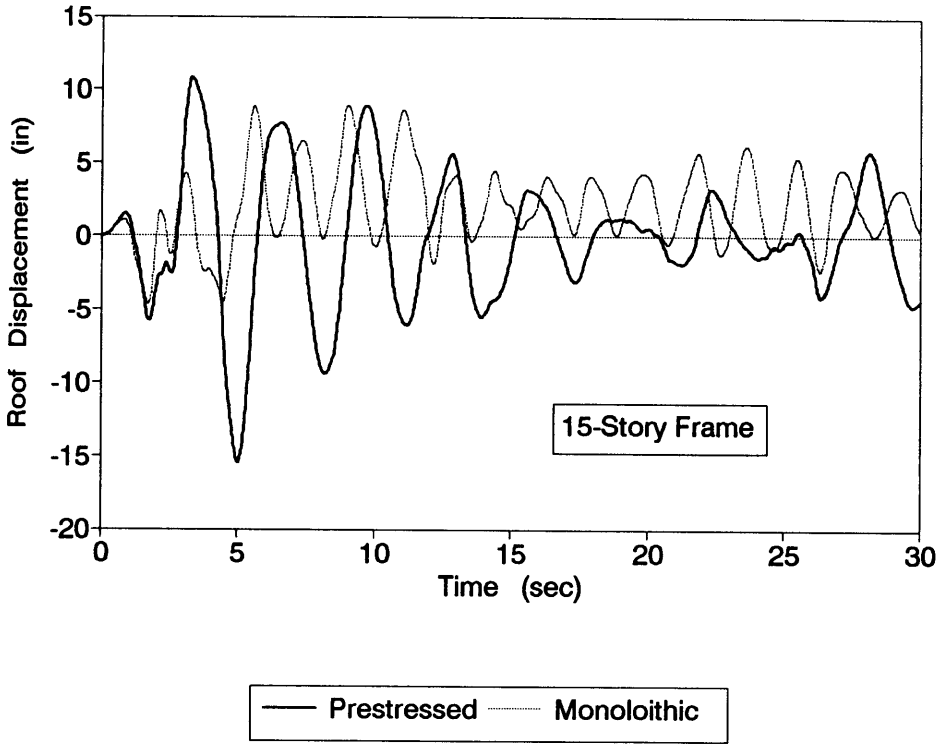

Fig. 30—Computed roof-level displacement response for fifteen-story frame subjected to 1940 El Centro